Fretting wear behavior of duplex PEO/chameleon coating on Al alloy

Yan-Fei Liu[1,2], Tomasz Liskiewicz[1], Aleksey Yerokhin[3], Andras Korenyi-Both[4], Jeffrey Zabinski[5], Mengyu Lin[3], Allan Matthews[3] and Andrey A. Voevodin[6]

[1]School of Mechanical Engineering, University of Leeds, Leeds LS2 9JT, UK

[2] Harbin Engineering University, Harbin, 150001, China

[3]School of Materials, University of Manchester, Manchester, M1 3BB, UK

[4] Colorado School of Mines, Dept. of Metallurgical & Materials Engineering, Golden, CO 80401, USA

[5]Army Research Laboratory, Aberdeen Proving Grounds, MD, 21005, USA

[6]Dept. of Materials Science and Engineering, University of North Texas, Denton, TX 76203, USA

Abstract

Plasma electrolytic oxidation (PEO) is an attractive technology for improving resistance to wear, heat and corrosion of aluminum alloys. PEO results in a hard, well-adhered alumina ceramic coating with a morphology which is graded from a dense region near the substrate interface to a porous outer region. Such properties mean that PEO can be an ideal underlying layer for the application of solid lubricants which can be entrapped in outer pores and provide reservoirs for the tribological contact lubrication. This study investigates the fretting wear behavior and adaptive mechanisms for a PEO-produced alumina surface of about 11-12 GPa hardness with a top layer of an $MoS_2/Sb_2O_3/C$ chameleon solid lubricating coating, the

composition of which was designed to self-adapt in variable humidity environments for friction and wear reduction. Coupons of AA 6082 alloy were coated by the PEO process and then were over-coated by a burnishing process with a $MoS_2/Sb_2O_3/C$ chameleon coating to prepare a duplex coating combination. The coated surfaces were investigated using nanoindenation, Raman spectroscopy and scanning electroscopy and were then subjected to fretting wear tests against steel and alumina balls with variable amplitude (0-100 micron) and loads (10-100 N) in both humid air and in dry nitrogen environment conditions. The tests demonstrated low friction coefficients, considerable reduction in critical amplitude for the stick-slip transition, and self-adaptive tribological behavior in cycled environment tests. Friction coefficients of the order of 0.10-0.15 in humid air and 0.06-0.09 in dry nitrogen were recorded and linked with the surface self-adjustment from graphite to MoS_2 lubrication, respectively, which was confirmed by Raman spectroscopy. The studies demonstrate the effectiveness of the PEO/chameleon duplex coating system for the friction reduction of and fretting wear in the gross-slip regime, as well as significantly reducing the critical amplitude of stick-slip transition for fatigue wear mitigation.

Keywords: Plasma electrolytic oxidation; Chameleon coating; Fretting; Wear, Tribology

1. Introduction

Owing to their low density and high strength-to-weight ratio, light metals, including aluminum, magnesium and titanium alloys, are widely used in aerospace, automotive and rail transportation applications, for example to reduce fuel consumption [1, 2]. These alloys are also used in the biomedical industry, for example; Ti6Al4V alloy is a commonly used implant material due to its low density, high corrosion resistance and biocompatibility [3, 4]. However, light alloys have poor sliding, rolling and fretting wear performance owing to their low hardness [5, 6] and absence of a low cycle fatigue limit. Recently, with the widening of light alloy applications, including engines, and aerospace components, it's becoming more important to enhance the surface performance of light alloys using surface treatments. Surface engineering of light alloys remains a challenge because they cannot be hardened effectively, while surface oxides can decrease the bonding between applied hard coatings and the substrate [1].

Plasma electrolytic oxidation (PEO) is an electrochemical surface treatment process for generating oxide coatings on metals [7-13]. PEO coatings have relatively high hardness and good adhesion strength to the substrate [8]. They typically consist of a porous outer layer, dense intermediate layer and thin inner layer [13]. PEO coatings are typically used to enhance the biocompatibility [7], thermal stability [9], friction and wear resistance, together with corrosion resistance [13].

They have been commonly used in engineering applications to enhance the tribological performance of aluminum alloys. The unlubricated sliding performance of PEO coatings in nitrogen, vacuum, 50%-humid air and 80%-humid air conditions were studied by Yerokhin et al. [14, 15]. It has been shown that external environment and humidity has a significant influence on the friction behavior of PEO coating. The existence of water in the air can enhance the formation of aluminum hydroxide at the contact interface, which leads to the reduction of

friction. As expected, compared to the untreated aluminum alloy substrate, PEO coatings shown better sliding wear resistance performance owing to the relatively high hardness [13]. Such wear resistance enhancement and a relatively low cost of the process has resulted in several industrial applications of PEO coatings on aluminum alloy surfaces for sliding wear reduction, but the studies of PEO coatings in fretting wear are limited [16, 17].

Fretting is a small amplitude oscillatory motion wear process between two bodies leading to progressive surface damage by inducting sub-surface material transformations [18]. Depending on the interfacial sliding behavior, fretting can be divided into two regimes; gross-slip condition when full sliding is observed at the interface, and stick-slip condition when no sliding occurs in the center of the contact and material is subjected to repeated elastic deformation cycles while the contact edges have low amplitude sliding [19, 20]. The stick-slip regime is especially critical in engineering applications with light weight alloys, since elastic deformation cycles in fretting wear contacts can lead to the onset of fatigue surface cracks and catastrophic component failure. Under gross sliding fretting wear, the interface firstly goes through plastic deformation followed by wear debris formation and detachment from the bulk material [21-23]. These debris are abrasive and lightweight materials can experience a significant wear due to their relatively low surface hardness. To counter both fretting wear regimes, contradicting requirements of a low shear strength surface (to prevent stick-slip and associated fatigue) and a high shear strength surface (to resistant abrasion) could be provided by duplex surface treatments and coatings to provide a low shear and soft top surface and high shear strength and hard underlying layer [24]. Several examples of such a combination can be found in the literature for fretting wear mitigation, including CrN/CuNiIn coating [25] and TiN/MoS_2 coating [26]. One common drawback is the absence of a resupply possibility and environmental adapting capability, which calls for the design and cost effective manufacturing

of hard surfaces where environmentally self-adaptive solid lubricants can be stored and released to the fretting wear contacts.

Solid lubricants are widely used in the aerospace engineering because of the extreme environment conditions, such as low or high temperatures, low pressures, variable humidity, and the presence of oxidants [27], which prevent the use or reduces the performance of traditional oil lubrication. However, a major challenge for solid lubricants in aerospace applications is humidity and temperature variations [28, 29]. For example, graphite can effectively reduce friction and wear in humid environments but has poor performance in dry or vacuum conditions [30]. The coefficient of friction and wear rate of MoS_2 are low in dry or vacuum conditions, but relatively high in humid conditions [31]. Aimed at this problem, the concept of adaptable chameleon coating was introduced, which provides self-lubrication [32-37], high surface hardness [38, 39] and good wear resistance performance in varied environments [40].

Chameleon coatings may have good self-lubrication performance and environmental adaptability, but relatively poor adhesion and low surface hardness, which can reduce their performance in fretting wear applications. Meanwhile, PEO coatings on lightweight aluminum and titanium alloys have excellent load support properties, which makes them a very good candidate for supporting sub-layer for chameleon coatings on lightweight alloys. Furthermore, the outer layer of the PEO coating has a high porosity, while the inner layer of the PEO coating has lower wear rate due to its relatively high hardness and low porosity [8]. Typically, the outer porous layer of the PEO coating is removed by mechanical polishing. However, in view of the combination with chameleon solid lubricant such a structure can be beneficial to provide lubricant reservoirs for their extended release into the fretting contact. To investigate such an approach for fretting wear mitigation, a new duplex PEO/chameleon ($MoS_2/Sb_2O_3/C$) coating was processed on AA 6082 series alloy substrates. The friction and wear performance of PEO

coating and PEO/chameleon coating were investigated under fretting conditions in humid air and dry nitrogen environment.

2. Methods

2.1 Materials

Substrates were made of aluminum alloy 6082. The samples were 50 mm by 50 mm squares of 1.5 mm thickness on one surface of which a PEO coating of about 20 µm thickness was prepared using experimental approaches as described in Ref [41]. For this purpose, a dilute alkaline electrolyte with additions of 1 to 2 g/l of Na_2SiO_3 and 2 to 3 g/l of $Na_4P_2O_7 \cdot 10H_2O$ was used. A pulsed bipolar polarization at a frequency of 1.7 kHz with fill factor of 0.4 and magnitudes of positive and negative bias of +530V and -180V respectively was utilized to achieve an initial RMS current density of about 30 A/dm^2; this provided a coating growth rate of 2 to 3 µm/min. The chameleon coating, which consists of a few micrometers of graphite doped with MoS_2 and Sb_2O_3 was burnished onto the surface of the PEO coating, following procedures described in Ref. [42]. For this purpose, chemically pure powders of graphite (40 wt %), MoS_2 (40 wt.%) and Sb_2O_3 (20 wt.%) were mixed and then hand burnished on the PEO sample surface using a lint free cloth to help smoothen the top layer surface. The burnishing process created about 5-8 µm thickness of MoS_2/Sb_2O_3/C composite overcoat on the surface of the PEO coating. PEO coating hardness and elastic moduli were measured by nanoindentations in a coating cross-section, which avoided the substrate influence. Indentations were performed with a Keysight G200 nanoindentor using a Berkovich tip with depth limit of 400 nm, following general procedures available in the literature [43]. Results were averaged over 120 indents conducted with a 0.15 nm/s allowable drift rate and 10 seconds of the maximum depth holding time. A fused silica test sample was used to calibrate the system compliance and the indentor area function.

2.2 Experimental setup

The tribological behavior of PEO and PEO/chameleon coatings was investigated with a ball-on-plane fretting test under different environmental conditions. An electro-dynamic powered fretting setup built in the School of Mechanical Engineering at the University of Leeds was used in this study [44]. During fretting tests, the coated sample was fixed in the static holder while the counter-body ball was fixed on the reciprocating arm. The normal load was applied with dead weights, previously calibrated with a load cell. The laboratory temperature was 22°C and relative humidity between 40% and 55%. Alumina balls 16mm in diameter and 440 stainless steel balls 12 mm in diameter were used in this study.

During the fretting tests, tangential force and displacement amplitude were recorded for each fretting cycle, using a calibrated load cell and a fiber optic displacement sensor respectively. All fretting tests were divided into three groups to investigate different tribological behavior under fretting wear. In the first group, a relatively high normal load and small amplitude were applied to investigate the transition between stick-slip and gross-slip conditions.

The alumina and steel balls used in this study had different diameters, elastic modulus and Poisson's ratios, and therefore normal loads were selected to match the Hetzian contact pressures to allow result comparisons. In the first group fretting tests, 100 N load was applied to the alumina ball and 75 N load was applied to the steel ball to provide contact pressures of 1680 MPa and 1664 MPa, respectively. For the contact pressure estimations, the elastic moduli of the PEO coated surface was assumed to be at 200 GPa, which was within the measured values reported below. While the estimate of the Hertzian contact pressure at about 1.6 GPa as provided here is approximate, due to PEO coating elastic moduli variation and a possibility of aluminum alloy substrate flexing under 20 μm thick PEO coating, this is representative of pressures encountered in practice for mechanically loaded bearings and other contacts.

Importantly, it was kept consistent in all tests reported here for the relative comparisons. The fretting test in group 1 experiments was designed in a way that the displacement amplitude was gradually decreased from ±100 μm until reaching a critical transition condition between gross-slip and stick-slip regimes.

In the second group, fretting tests were conducted to investigate the tribological performance of PEO and PEO/chameleon coatings at different environment conditions, including humid air and dry nitrogen. For all fretting tests in group 2, the frequency was 3 Hz to reduce the test duration. The amplitude was 100 μm to ensure that all tests are at gross-slip condition. For the alumina ball and the steel ball, the normal loads were 20 N and 15 N respectively to minimize the difference in initial contact pressures, which were at 980 MPa and 1070 MPa respectively.

A two-piece retractable chamber was designed to create an isolated environment for the nitrogen test. A flexible tube was inserted into the chamber, which was then filled with dry nitrogen for 45 min before fretting to assure stable environmental conditions. Dry nitrogen was continuously pumped during the fretting tests to avoid the humidity rise. A hygrometer probe was inserted inside the chamber to monitor the humidity level.

In the third group of fretting tests, all the parameters were the same as in the second group except the fretting test duration. In the third group, 100,000 cycle fretting tests were conducted to investigate the performance of PEO and PEO/chameleon coatings under long-term fretting wear. Detailed parameters of group 1-3 tests can be seen in Table 1.

2.3 Surface characterization

2.3.1. Wear volume measurements

A white light non-contact profilometry (Bruker NPFLEX) was utilized to characterize the wear scars of PEO and PEO/chameleon coatings. This method was used to obtain a qualitative 3D surface morphology and quantitative assessment of wear depth. Comparing to the

PEO/chameleon coating, the surface morphology of PEO coating was more difficult to characterize due to the high surface porosity. Therefore, the surface scanning method for PEO coating was set at 10× magnification and 1× scanning speed to capture many data points, while the scanning for PEO/chameleon coating was set at 10× magnification and 3× scanning speed to reduce the scanning time. The scanning area for all the samples was 1.5×1.5 mm^2.

2.3.2. SEM imaging

The microstructure and composition of PEO and PEO/chameleon coatings were investigated with a scanning electron microscopy (SEM, Zeiss EVO50 VPSEM) which was equipped with an X-ray energy dispersive spectrometer (EDS). The accelerating voltage and working distance for SEM tests were 20 kV and 17.5 mm, respectively. A focused ion beam-scanning electron spectrometer microscope (FIB-SEM, FEI Quanta 3D), which was operated under 5 kV accelerating voltage and 10 mm working distance, was used for further visualization of the microstructure of the chameleon coating. To eliminate the charge distribution phenomenon and enhance the conductivity of the sample, an approximately 10 nm thicknesses of platinum layer was deposited on the surface of the test samples.

2.3.3. Raman characterization

Raman spectra of the wear scars were obtained using a Renishaw System 1000 Raman spectrometer utilizing an Argon-ion laser (λ = 514.50 nm) as the excitation source. The spectrometer was calibrated against Si peaks at 520 cm^{-1} provided by a plane silicon wafer crystal. The spectra were taken from regions with surface area of several μm^2 located within the wear scars, as identified by an optical microscope attached to the spectrometer. A reference spectrum was also taken from the sample region not subjected to the wear tests. The relative density of basal to edge sites in MoS_2 was estimated using intensities of E_{2g} and A_{1g} bands at

383 and 408 cm^{-1} respectively [45]. The average size of in-plane crystallite size of graphite phase was estimated from integrated intensities (areas) of D and G bands (I_D and I_G) located respectively at 1355 and 1580 cm^{-1} using the following equation [46];

$$L_a = (2.4x10^{-10}) \cdot \lambda^4 (I_D/I_G)^{-1}$$

Where La (nm) is the average size of sp^2 crystallite clusters and λ is the excitation laser wavelength (nm).

3. Results and discussion

3.1. Surface morphology

Figure 1 a shows an SEM image of an as-produced PEO coating where a micron scale rough morphology with a degree of surface porosity can be clearly seen. Such a morphology results from the stochastic motion of surface arc discharges during the coating process, which converts the aluminum alloy surface into ceramic alumina coating and is typical for PEO processing [41]. The surface roughness of as-produced PEO coatings was measured at an Ra value of about 2.7 μm. Such roughness and porosity (visible in Figure 1a) was used to mechanically bond and create reservoir sites for the chameleon burnished coating applied as the next processing step. After the chameleon overcoat application, the sample surface morphology was much smoother, as evidenced in Figure 1b. Correspondingly, the surface roughness was reduced to an Ra value of about 0.2-0.3 μm. Figure 1b also indicates macroscopic variations in chameleon coating thickness with visible thicker patches of the burnished chameleon coating. Since a chameleon coating is very soft, the thickness non-uniformity was not deemed critical for the fretting wear studies as it was expected that the contact pressure will extrude the excess of chameleon overcoat and the load will be fully supported by the relatively harder PEO alumina coating.

Figure 2 presents a cross-sectioned image of the PEO/chameleon coating, where the layers of the alumina and chameleon coating are clearly visible, allowing for the estimations of thecoating layer thicknesses. It is clear that the chameleon coating is conformal to the PEO surface, covering up the PEO surface rough morphology. The images also illustrate the fully dense nature of the inner regions of the PEO coating, which is important observation for the coating mechanical endurance reported later. Nanoindentation experiments performed on the PEO coating cross-section had indicated that both the hardness and elastic moduli fluctuate in a wide range, where the hardness value of the PEO coating was varied in the 10-33 GPa range, and the corresponding elastic moduli were varied within the 165-370 GPa range over 20 measurements. Such a large variation of the measured nanoindentation response and the presence of harder (α-Al_2O_3) and softer (β-Al_2O_3) phases was reported on previously [47, 48]. The chameleon solid lubricating overcoat is very soft and is easily pushed out of the contact. It therefore doesn't contribute to the load support during the fretting wear contact. Nevertheless, the presence of the MoS_2, Sb_2O_3, and graphite phases with low shear strength in the chameleon overcoat layer is critical for the observed fretting wear response which is discussed in detail in the following sections.

3.2 Friction behavior

A fretting loop is a commonly used method to identify the fretting contact response [49, 50]. The tangential force versus displacement amplitude loops of fretting tests under 75 N normal load on PEO coating (a-b), and PEO/chameleon coating (c-d) against steel ball in air condition are plotted in Figure 3. The detailed transition amplitudes between stick-slip and gross slip fretting regimes are shown in Table 2. Fretting loops shown in Figure 3 (a) and (c) exhibit a characteristic narrow shape for stick-slip regime, while loops shown in Figure 3 (b) and (d) have a fraction parallel to the displacement axis indicating a full sliding events at the

ball/coating interface and associated with the gross-slip fretting regime [51, 52]. Based on the fretting regime transition amplitudes shown in Table 2, it can be concluded that the transition between stick-slip and gross-slip regimes for the PEO/chameleon coating happened at much lower amplitudes than for PEO coating. This is very beneficial for reducing occurrence of the stick-slip regime in practical applications and corresponding fatigue crack developments [19,20].

Under gross-slip condition in fretting, the ratio between tangential force and applied normal load can be extracted from the loop and interpreted as an indication of coefficient of friction (CoF) [49]. The evolution of CoF for PEO and PEO/chameleon coatings during 10,000 cycles fretting tests against steel in air and nitrogen are plotted in Figure 4. It can be observed that the CoF for PEO coating against steel is higher than that of PEO/chameleon coating in both, air and nitrogen conditions. The friction reduction mechanism of the $MoS_2/Sb_2O_3/C$ chameleon coating was explained by Zabinski et al. [42]. In the chameleon composite coating, graphite acts as lubricant in humid environment while MoS_2 acts as lubricant in a dry nitrogen environment. Meanwhile, Sb_2O_3 acts synergistically with MoS_2 to further improve the friction behavior of the chameleon coating. In nitrogen atmosphere, the CoF is lower than that observed in air for both, PEO and PEO/chameleon coatings. Oxidation of MoS_2 film forms MoO_3 phases that have a negative effect on lubricant performance. MoO_3 can display reasonably low CoF among oxides but not nearly as low as that of MoS_2 [53]. In this study, the dry nitrogen environment restrained the formation of MoO_3, which resulted in low friction performance of MoS_2. Moreover, fretting wear process against a steel ball generates oxidized wear debris in a humid air [54], which leads to higher coefficient of friction on PEO coatings [8]. The lubrication performance of MoS_2 in dry nitrogen is better than that of graphite in humid air due to synergistic effects with Sb_2O_3 [55], which leads to lower CoF of chameleon coatings in dry nitrogen condition compared to humid air environment.

In the case of fretting contact against an alumina ball, the evolution of CoF for PEO and PEO/chameleon coatings during 10,000 cycles fretting tests in air and nitrogen environments are plotted in Figure 5. It can be observed that the CoF for the PEO coating against alumina is much higher than that for the PEO/chameleon coating in both air and nitrogen owing to the self-lubricating performance of the chameleon coating, which is the same effect as observed in the fretting contact against the steel ball. The PEO/chameleon coating also showed lower CoF in nitrogen than in air due to superior the lubrication behavior of MoS_2. However, the CoF for the PEO coating in dry nitrogen is significantly higher than that in humid air, which is different from the results obtained against steel. This can be attributed to the fact that a thin lubricating film of aluminum hydroxide is formed in a humid environment at the alumina/PEO coating interface [8]. Average coefficient of friction values for tested coatings against steel and alumina balls in air and nitrogen atmospheres are listed in Table 3.

Fretting experiments for 100,000 cycles were conducted to investigate the long-term frictional behavior of tested coatings in air (Figure 6) and nitrogen (Figure 7). It has been shown that during tests in air against steel the CoF for the PEO coating would stay at a high level (between 0.95 and 1.00) during the entire fretting test, while CoF for the PEO/chameleon coating would gradually increase at the early stage, then stay stable at around 0.92 after 20,000 cycles fretting. Interestingly, the CoF for the PEO/Chameleon coating against alumina remained at around 0.22 until 25,000 fretting cycles, after which it gradually increased to around 0.68. In humid air environment condition, graphite acted as an active lubricant, dominating the lubrication performance of $MoS_2/Sb_2O_3/C$ chameleon coating. During the fretting process, Sb_2O_3 phase provided a lubrication effect maintaining low friction performance. Previous research defined failure of $MoS_2/Sb_2O_3/C$ coating as an increase in average friction over 0.65 [42]. Hence, in this study the significant increase of CoF observed in air environment (Figure 6) is interpreted as the failure of the chameleon coating.

In the case of a nitrogen environment, the evolution of CoF for PEO coating against steel would stay constant at approximately 0.90-0.98, while for PEO/chameleon the observed CoF was much lower at around 0.15-0.22. The friction of PEO/chameleon coating against alumina had a decreasing trend with CoF at 0.17 at the beginning of the test and 0.13 after 100,000 fretting cycles. Hence, the PEO/chameleon coating can significantly reduce the friction and improve wear performance in both humid air and dry nitrogen conditions owing to the lubricating properties of graphite and MoS_2. The presence of hexagonal MoS_2 and graphite in the contact region is verified with Raman spectroscopy analysis discussed in section 3.4.

3.3 Wear performance

Wear volume is typically used as a key parameter to characterize wear performance of materials. However, in this study, a relatively rough nature of PEO/chameleon coating surface made it difficult to calculate the wear volume accurately. For this reason, wear depth was used instead in this study. Examples of 3D surface morphologies and wear depth measurements of tested coatings against steel and alumina in air and nitrogen are shown in Figure 8 and summarized in Table 4. It can be observed that the wear depth of the PEO coating against steel is larger than that of the PEO coating against alumina in both air and nitrogen conditions. The wear depth of the PEO coating against steel in air is larger than in nitrogen while the wear depth of the PEO coating against alumina in air is smaller than in nitrogen. In the case of the PEO/chameleon coating, the wear depth is smaller under a nitrogen environment. Meanwhile, the wear depth of the PEO/chameleon coating against steel is larger in air environment while the wear depth against alumina is smaller in air. The larger wear against a steel counterpart in air is mostly caused by entrapped debris from wear and oxidation of the steel counterpart. Accumulations of debris and oxides in the contact zone are important considerations for fretting wear and may explain the observed differences in wear depths for tests with alumna and steel

balls in air. In general, the PEO coating showed lower wear resistance in all test conditions which results from its lower hardness and relatively high porosity [8].

Meanwhile, the improved wear performance of the $MoS_2/Sb_2O_3/C$ chameleon coating can be attributed to the properties of each individual component as well as the synergism between the phases. MoS_2 has relatively high wear resistance owing to its crystallographic structure and well-defined plane consisting of a transfer film containing basal-oriented MoS_2. However, the wear resistance of MoS_2 decreases in oxidizing atmosphere due to a non-cohesive transfer film formation, which leads to continuous loss of material from the contact region and accelerated wear [56]. The presence of graphite enhances the wear resistance of MoS_2 by facilitating the inter-crystalline slip and diffusion barrier formation [57]. Moreover, addition of Sb_2O_3 phase prevents oxidation deeper into the coating and reduces the tribo-oxidation effects. Sb_2O_3 also acts as an effective supportive layer for MoS_2 [58, 59], which enhances the overall wear performance of the chameleon coating. Owing to the synergistic effects between its phases, the chameleon coating has better wear resistance than pure graphite and hexagonal MoS_2 films [42].

3.4 Structural evolution of Chameleon coating due to fretting

Raman spectra taken from wear scars developed on the PEO/chameleon coatings as a result of 10,000 cycles of fretting against steel and alumina in air and nitrogen are shown in Figure 9, together with the original spectrum of as deposited duplex coating.

The spectra feature clear peaks of vibration modes for hexagonal MoS_2 (E_{2g} 383 cm^{-1} and A_{1g} 408 cm^{-1}) and graphite (D 1355 cm^{-1} and G 1580 cm^{-1}). The response from the Sb_2O_3 phase and underlying PEO alumina cannot not be reliably identified, although some broad and weak bands could be observed at about 150-250, 400-480, 550-650, 720-800 and 1100-1200 cm^{-1}. Strongest peaks of Sb_2O_3 normally appear around 250 and 450 cm^{-1}. While there is some

indication of their presence, this is very minor as compared to the dominant MoS_2 and graphite peaks, indicating an absence of well-defined Sb_2O_3 phases. Among relevant alumina polymorphs, only rhombohedral α-Al_2O_3 (corundum) is Raman active, providing peaks in the studied spectral range at about 420 and 650 cm^{-1}. However this phase is mainly formed the inner parts of the PEO coating located beneath the region probed by the Raman analysis.

As follows from Figure 9, the fretting tests do not induce any qualitative changes in the Raman spectra of the studied surfaces, implying that both MoS_2 and graphite solid lubricant components of the chameleon layer remain present in the fretting contact area. However the relative intensities of the major peaks change. The intensity ratio of MoS_2 E_{2g} to A_{1g} bands can be used to estimate the relative density of basal and edge sites in MoS_2 [45]. While, the intensity ratio I_D/I_G of the two graphite bands could also be utilized to evaluate the average size of in-plane crystallite size L_a in graphite [46]. Evaluated characteristics of MoS_2 and graphite phases are provided in Table 5. It can be seen that fretting tests cause the average size of graphite clusters within the chameleon coating to increase slightly from about 15 nm to 16-17.5 nm, besides the increase is more prominent following the tests in air. The Mo_2S phase appears to align mainly along the basal planes, which is signified by the values of E_{2g}/A_{1g} ratio above 0.8. This observation is consistent with previously reported results of transmission electron microscopy analysis which revealed development of preferred orientations of MoS_2 and graphite basal planes parallel to the surface in similar chameleon coatings under sliding wear conditions [42]. In fretting wear contacts of this study, the graphite phase surface alignment (L_a parameter in Table 5) increased noticeably for the tests in air as compared to the tests in nitrogen, and had very little dependence on the counterpart material. At the same time, the MoS_2 phase alignment (E_{2g}/A_{1g} ratio in Table 5) change depended on both environment and counterpart material. It showed a reduction in MoS_2 basal plane parallel orientations for tests against alumina in humid air, while maximum enhancement of such orientation was

observed for the tests against steel in the dry nitrogen. Overall Raman analysis results corroborate previous reports of the adaptive behavior of chameleon coatings [32], but fretting wear adaptive mechanisms may vary from those of the sliding tests. Explorations of such mechanisms for duplex PEO/chameleon coatings can further enhance fretting wear resistance of light weight metal alloys surfaces.

4 Conclusions

A cost effective and scalable process for preparing duplex PEO/chameleon coatings on the surface of lightweight aluminum alloy was shown to provide a unique combination of the hard abrasion wear resistant underlying surface made of aluminosilicate oxides and a low shear top surface of environmentally adaptive $MoS_2/Sb_2O_3/C$ chameleon coating solid lubricant. The chameleon surface lubricant was embedded by filling the residual porosity (typical for the PEO process) of the top oxide layer with a simple burnishing process. The elastic moduli and hardness of the underlying PEO layer was varied within 165-370 GPa and 10-33 GPa, respectively, which in the combination of about 20 μm thickness provides necessary contact load support and abrasion resistance for fretting wear resistance. The cross-sectional SEM studies had confirmed such duplex coating morphology where about 5-8 μm thick solid lubricant layer was embedded in with PEO surface, which porous about 3 μm R_a roughness morphology was completely filled by the burnished chameleon coating. Raman spectroscopy had clearly indicated the presence of hexagonal MoS_2 and graphite solid lubricant phases on the coating surface, which related to the observed reduction of the friction coefficients and also the critical stroke amplitude for the transition from gross to stick-slip fretting regime, when tested against steel and alumina counterparts in humid air and dry nitrogen conditions. Friction coefficients of order of 0.10-0.15 in humid air and 0.06-0.09 in dry nitrogen were recorded and linked with the surface self-adjustment from graphite to MoS_2 lubrication, respectively. Critical

amplitudes for transition to stick-slip behavior against steel counterpart were reduced from 40-50 μm for steel/PEO coating tests to 2-5 μm for steel/PEO+chameleon duplex coating test. Such an order of magnitude reduction was accompanied also with about a factor two improvement in wear volume reduction. The study demonstrates the effectiveness of the PEO/chameleon duplex coating system benefit for the friction loss and fretting wear reduction in gross-slip regime and fatigue wear mitigation for small stroke regimes under humid and dry conditions and against steel and ceramic counterparts.

Acknowledgements

Andrey A. Voevodin acknowledges support from Distinguished Visitor Programme of UK Royal Society DVP and Cooperative Agreement between the Army Research Laboratory and the University of North Texas (W911NF-13-2-0018). Aleksey Yerokhin, Mengyu Lin and Allan Matthews acknowledge financial support from the ERC Advanced Grant (#320879“IMPUNEP”). Yanfei Liu acknowledges support from Harbin Engineering University Scholarship Fund (No. 201603).

References

[1] H Dong, Surface engineering of light alloys: aluminum, magnesium and titanium alloys, Elsevier, Amsterdam, 2010.

[2] M. Peters, J. Kumpfert, C. H. Ward, C. Leyens, Titanium alloys for aerospace applications, Advanced Engineering Materials, 5 (2003) 419-427.

[3] Rinner, M., J. Gerlach, W. Ensinger, Formation of titanium oxide films on titanium and Ti6Al4V by O_2-plasma immersion ion implantation, Surf. Coat. Technol. 132 (2000), 111-116.

[4] D. E. MacDonald, B. E. Rapuano, N. Deo, M. Stranick, P. Somasundaran, A. L. Boskey, Thermal and chemical modification of titanium–aluminum–vanadium implant materials: effects on surface properties, glycoprotein adsorption, and MG63 cell attachment, Biomaterials 25 (2004) 3135-3146.

[5] A. Molinari, G. Straffelini, B. Tesi, T. Bacci, Dry sliding wear mechanisms of the Ti6Al4V alloy, Wear 208 (1997) 105-112.

[6] S. Wilson, A. T. Alpas, Effect of temperature on the sliding wear performance of Al alloys and Al matrix composites, Wear 196 (1996) 270-278.

[7] X. Lu, M. Mohedano, C. Blawert, E. Matykina, R. Arrabal, K. U. Kainer, M. L. Zheludkevich, Plasma electrolytic oxidation coatings with particle additions–A review, Surf. Coat. Technol. 307 (2016) 1165-1182.

[8] A. L. Yerokhin, X. Nie, A. Leyland, A. Matthews, S. J. Dowey, Plasma electrolysis for surface engineering, Surf. Coat. Technol. 122 (1999) 73-93.

[9] J. A. Curran, T. W. Clyne, Thermo-physical properties of plasma electrolytic oxide coatings on aluminum, Surf. Coat. Technol. 199 (2005) 168-176.

[10] E. Matykina, A. Berkani, P. Skeldon, G. E. Thompson, Real-time imaging of coating growth during plasma electrolytic oxidation of titanium, Electrochim. Acta 53 (2007) 1987-1994.

[11] S. Yagi, K. Kuwabara, Y. Fukuta, K. Kubota, E. Matsubara, Formation of self-repairing anodized film on ACM522 magnesium alloy by plasma electrolytic oxidation, Corrosion Sci. 73 (2013) 188-195.

[12] S. V. Gnedenkov, O. A. Khrisanfova, A. G. Zavidnaya, S. L. Sinebrukhov, P. S. Gordienko, S. Iwatsubo, A. Matsui, Composition and adhesion of protective coatings on aluminum, Surf. Coat. Technol. 145 (2001) 146-151.

[13] X. Nie, E. I. Meletis, J. C. Jiang, A. Leyland, A. L. Yerokhin, A. Matthews, Abrasive wear/corrosion properties and TEM analysis of Al_2O_3 coatings fabricated using plasma electrolysis, Surf. Coat. Technol. 149 (2002) 245-251.

[14] A. L. Yerokhin, A. A. Voevodin, V. V. Lyubimov, J. Zabinski, M. Donley, Plasma electrolytic fabrication of oxide ceramic surface layers for tribotechnical purposes on aluminum alloys, Surf. Coat. Technol. 110 (1998) 140-146.

[15] A.L. Yerokhin, A.A. Voevodin, V.V. Lyubimov, and M. Donley J.S. Zabinski, Tribological Properties of Oxide Ceramic Coatings on Al Alloy Produced by Microarc Discharge Oxidation, SET'97, Proceed. of All-Russian Conf., Tula, TulGU (1997) 239-246

[16] M. H. Zhu, Z. B. Cai, X. Z. Lin, P. D. Ren, J. Tan, Z. R. Zhou. Fretting wear behaviour of ceramic coating prepared by micro-arc oxidation on al–si alloy, Wear 263 (2007) 472-480.

[17] M. H. Zhu, Z. B. Cai, X. Z. Lin, J. F. Zheng, J. Luo, Z. R. Zhou. Fretting wear behaviors of micro-arc oxidation coating sealed by grease, Wear 267 (2009) 299-307.

[18] T. Liskiewicz, K. Kubiak, T. Comyn, Nano-indentation mapping of fretting-induced surface layers, Tribol. Int. 108 (2017) 186–193.

[19] O. Vingsbo, S. Söderberg, On fretting maps, Wear 126 (1988) 131-147.

[20] P. L. Hurricks, The mechanism of fretting—a review, Wear 15 (1970) 389-409.

[21] R. B. Waterhouse, Fretting wear, Wear 100 (1984) 107-118.

[22] E. Sauger, S. Fouvry, L. Ponsonnet, P. Kapsa, J. M. Martin, L. Vincent, Tribologically transformed structure in fretting, Wear 245 (2000) 39-52.

[23] C. Paulin, S. Fouvry, S. Deyber, Wear kinetics of Ti–6Al–4V under constant and variable fretting sliding conditions, Wear 259 (2005) 292-299.

[24] K. Holmberg, A. Matthews, Wear: Materials Mechanisms and Practice, in: G. W. Stachowiak, Tribology of Engineered Surfaces, Wiley, Hoboken, 2006, pp. 123-166.

[25] D. Liu, B. Tang, X. Zhu, H. Chen, J. He, J. P. Celis, Improvement of the fretting fatigue and fretting wear of Ti6Al4V by duplex surface modification, Surf. Coat. Technol. 116 (1999) 234-238.

[26] G. Xu, Z. Zhou, J. Liu, X. Ma, An investigation of fretting behavior of ion-plated TiN, magnetron-sputtered MoS_2 and their composite coatings, Wear 225 (1999) 46-52.

[27] R. Team, Characterization of the Martian surface deposits by the Mars Pathfinder rover, Sojourner. Science 278 (1997) 1765-1768.

[28] T. Liskiewicz, S. Fouvry, B Wendler, R. Rybiak, Fretting wear of Ti(CxNy) PVD coatings under variable environmental conditions, Proc. IMechE Part J: Journal of Engineering Tribology 220 (2006) 125-134.

[29] A. A. Voevodin, J. P. O'neill, J. S. Zabinski, Nanocomposite tribological coatings for aerospace applications, Surf. Coat. Technol. 116 (1999) 36-45.

[30] H. E. Sliney, Solid lubricant materials for high temperatures—a review, Tribol. Int. 15 (1982) 303-315.

[31] J. K. Lancaster, Lubrication by transferred films of solid lubricants, ASLE transactions 8 (1965) 146-155.

[32] C. Muratore, A. A. Voevodin, Chameleon coatings: adaptive surfaces to reduce friction and wear in extreme environments, Ann. Rev. Mater. Res. 39 (2009) 297-324.

[33] A. A. Voevodin, J. S. Zabinski, Nanocomposite and nanostructured tribological materials for space applications, Compos. Sci. Technol. 65 (2005) 741-748.

[34] C. C. Baker, R. R. Chromik, K. J. Wahl, J. J. Hu, A. A. Voevodin, Preparation of chameleon coatings for space and ambient environments, Thin Solid Films 515 (2007) 6737-6743.

[35] A. A. Voevodin, J. S. Zabinski, Supertough wear-resistant coatings with “chameleon” surface adaptation, Thin Solid Films 370 (2000) 223-231.

[36] B. K. Yen, B. E. Schwickert, M. F. Toney, Origin of low-friction behavior in graphite investigated by surface x-ray diffraction, Appl. Phys. Lett. 84 (2004) 4702-4704.

[37] A. A. Voevodin, A. W. Phelps, J. S. Zabinski, M. S. Donley, Friction induced phase transformation of pulsed laser deposited diamond-like carbon, Diam. Relat. Mat. 5 (1996) 1264-1269.

[38] A. A. Voevodin, J. P. O’neill, J. S. Zabinski, Tribological performance and tribochemistry of nanocrystalline WC/amorphous diamond-like carbon composites, Thin Solid Films 342 (1999) 194-200.

[39] A. A. Voevodin, M. S. Donley, J. S. Zabinski, J. E. Bultman, Mechanical and tribological properties of diamond-like carbon coatings prepared by pulsed laser deposition Surf. Coat. Technol. 76 (1995) 534-539.

[40] K. J. Wahl, I. L. Singer, Quantification of a lubricant transfer process that enhances the sliding life of a MoS_2 coating, Tribol. Lett. 1 (1995) 59-66.

[41] A.L. Yerokhin, A. Shatrov, V. Samsonov, P. Shashkov, A. Pilkington, A. Leyland and A. Matthews, Oxide Ceramic Coatings on Aluminum Alloys Produced by a Pulsed Bipolar Plasma Electrolytic Oxidation Process, Surf. Coat. Technol. 199 (2005) 150– 157.

[42] J. S. Zabinski, J. E. Bultman, J. H. Sanders and J. J. Hu, Multi-environmental lubrication performance and lubrication mechanism of $MoS_2/Sb_2O_3/C$ composite films, Tribol. Lett. 23 (2006) 155-163.

[43] W. C. Oliver, G. M. Pharr, An improved technique for determining hardness and elastic modulus using load and displacement sensing indentation experiments, J. Mater. Res. 7 (1992) 1564-1583.

[44] K. J. Kubiak, T. W. Liskiewicz, T. G. Mathia, Surface morphology in engineering applications: Influence of roughness on sliding and wear in dry fretting, Tribol. Int. 44 (2011) 1427-1432.

[45] S. M. Tan, A. Ambrosi, Z. Sofer, Š. Huber, D. Sedmidubský, M. Pumera, Pristine basal- and edge-plane-oriented molybdenite MoS_2 exhibiting highly anisotropic properties, Chem.-Eur. J. 21 (2015) 7170–7178.

[46] L. G. Cançado, K. Takai, T. Enoki, M. Endo, Y. A. Kim, H. Mizusaki, A. Jorio, L. N. C. General equation for the determination of the crystallite size of nanographite by Raman spectroscopy, Appl. Phys. Lett. 88 (2006) 163106.

[47] A. A. Voevodin, A. L. Yerokhin, V. V. Lyubimov, M. S. Donley, J. S. Zabinski, Characterization of wear protective Al-Si-O coatings formed on Al-based alloys by micro-arc discharge treatment, Surf. Coat. Technol. 86 (1996) 516-521.

[48] R. H. U. Khan, A. L. Yerokhin, X. Li, H. Dong, A. Matthews, Surface characterisation of DC plasma electrolytic oxidation treated 6082 aluminum alloy: Effect of current density and electrolyte concentration, Surf. Coat. Technol. 205 (2010) 1679-1688.

[49] S. Fouvry, P. Kapsa, L. Vincent, Analysis of sliding behaviour for fretting loadings: determination of transition criteria, Wear 185 (1995) 35-46.

[50] T. Liskiewicz, S. Fouvry, B. Wendler, Impact of variable loading conditions on fretting wear, Surf. Coat. Technol. 163-164 (2003) 465-471.

[51] Z. R. Zhou, K. Nakazawa, M. H. Zhu, N. Maruyama, P. Kapsa, L. Vincent, Progress in fretting maps, Tribol. Int. 39 (2006) 1068-1073.

[52] S. R. Pearson, P. H. Shipway, Is the wear coefficient dependent upon slip amplitude in fretting? Vingsbo and Söderberg revisited, Wear 330 (2015) 93-102.

[53] P. D. Fleischauer, J. R. Lince, A comparison of oxidation and oxygen substitution in MoS_2 solid film lubricants, Tribol. Int. 32 (1999) 627-636.

[54] M. Godet, The third-body approach: a mechanical view of wear, Wear 100 (1984) 437-452.

[55] P. W. Centers, Tribological performance of MoS_2 compacts containing MoO_3, Sb_2O_3 or MoO_3 and Sb_2O_3, Wear 122 (1988) 97-102.

[56] I. L. Singer, S. Fayeulle, P. D. Ehni, Wear behavior of triode-sputtered MoS_2 coatings in dry sliding contact with steel and ceramics, Wear 195 (1996) 7-20.

[57] M. Gardos, The synergistic effects of graphite on the friction and wear of MoS_2 films in air, ASLE Transactions, 31 (1988) 214-227.

[58] P. Centers, The role of oxide and sulfide additions in solid lubricant compacts, ASLE Transactions, 31 (1988) 149-156.

[59] J. S. Zabinski, M. S. Donley, N. T. Mcdevitt, Mechanistic study of the synergism between Sb_2O_3, and MoS_2, lubricant systems using raman spectroscopy, Wear 165 (1993) 103-108.

Table 1. Parameters of the group 1-3 fretting tests.

Groups	Ball	Coatings	Frequency	Amplitude	Environment	Normal load	Cycles
Group 1	Alumina	PEO/chameleon	1 Hz	6 µm	Air	100 N	1,500
		PEO		12 µm		100 N	
	Steel	PEO/chameleon		4 µm		75 N	
		PEO		40 µm		75 N	
Group 2	Alumina	PEO	3 Hz	100 µm	Air	20N	10,000
		PEO/chameleon			N_2		
	Steel				Air	15N	
					N_2		
Group 3	Alumina	PEO	3 Hz	100 µm	Air	20N	100,000
		PEO/chameleon			N_2		
	Steel				Air	15N	
					N_2		

Table 2. Transition amplitudes between gross slip and stick/slip fretting regimes (75 N normal load).

	PEO against steel	PEO against alumina	PEO/chameleon against steel	PEO/chameleon against alumina
Stroke amplitude for stick-slip/ gross slip regimes (μm)	41.7/56.5	10.7/12.1	3.4/4.8	5.1/6.8

Table 3. Average coefficient of friction for tested coatings against steel and alumina balls in air and nitrogen atmospheres.

Fretting Wear System	Average CoF in air	Average CoF in nitrogen
PEO against steel	0.93	0.89
PEO against alumina	0.77	0.92
PEO/chameleon against steel	0.12	0.07
PEO/chameleon against alumina	0.11	0.08

Table 4. Wear depth values for tested coatings against steel and alumina in air and nitrogen.

	Maximum wear depth in air (μm)	Maximum wear depth in nitrogen (μm)
PEO against steel	11.5	7.2
PEO against alumina	2.1	5.1
PEO/chameleon against steel	6.6	2.9
PEO/chameleon against alumina	3.8	3.6

Table 5. Effect of fretting test conditions on the characteristics of graphite and MoS_2 solid lubricant phases in chameleon coating surface from Raman analysis.

Phase / Characteristic	Test Condition (Counterface / Environment)				
	As-deposited	Alumina/ N_2	Alumina/ Air	Steel / N_2	Steel / Air
In-plane Graphite phase size/ L_a(nm)	15.15	16.04	17.57	16.07	17.28
In plane Mo_2S orientation/ E_{2g}/A_{1g}	0.92	0.94	0.88	1.00	0.96

Figure 1. Surface topography (a) PEO coating, (b) PEO/chameleon coating.

Figure 2. SEM cross-section image of the PEO/chameleon coating on the surface of aluminum alloy sample.

Figure 3. Fretting loops against steel in humid air: (a-b) PEO coating, (c-d) PEO/chameleon coating.

Figure 4. Coefficient of friction evolution of PEO and PEO/chameleon coatings against steel under 10,000 cycles fretting with 15N normal load, 100μm amplitude and 3Hz frequency.

Figure 5. Coefficient of friction evolution of PEO and PEO/chameleon coatings against alumina under 10,000 cycles fretting with 20N normal load, 100μm amplitude and 3Hz frequency.

Figure 6. Coefficient of friction evolution of PEO and PEO/chameleon in air under 100,000 cycles fretting with 100μm amplitude and 3Hz frequency.

Figure 7. Coefficient of friction evolution of PEO and PEO/chameleon in nitrogen under 100,000 cycles fretting with 100μm amplitude and 3Hz frequency.

Figure 8. Worn surface morphology after 10,000 cycles. (a) PEO against steel in air, (b) PEO/Chameleon against steel in air, (c) PEO against alumina in air, (d) PEO/chameleon against alumina in air.

Figure 9. Raman spectra of PEO/chameleon coatings following fretting tests.

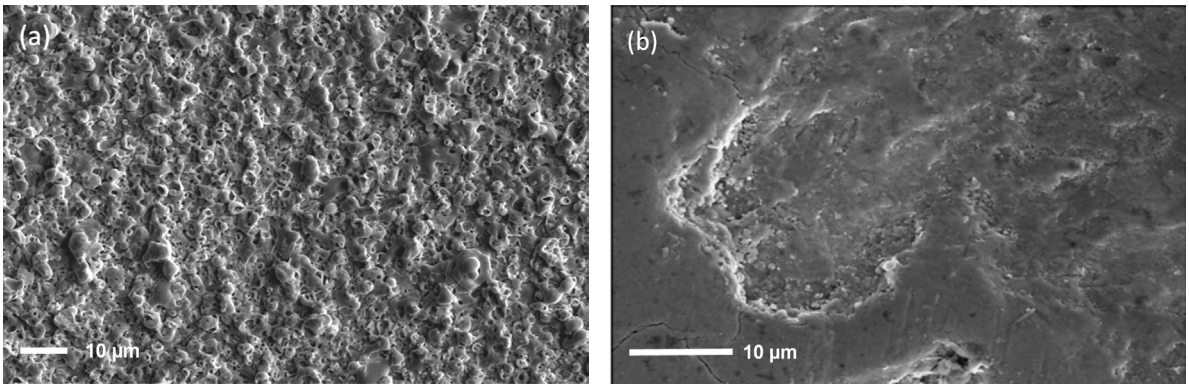

Figure 1

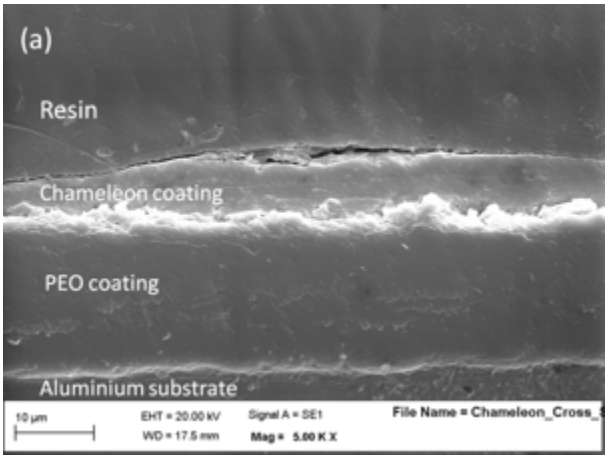

Figure 2

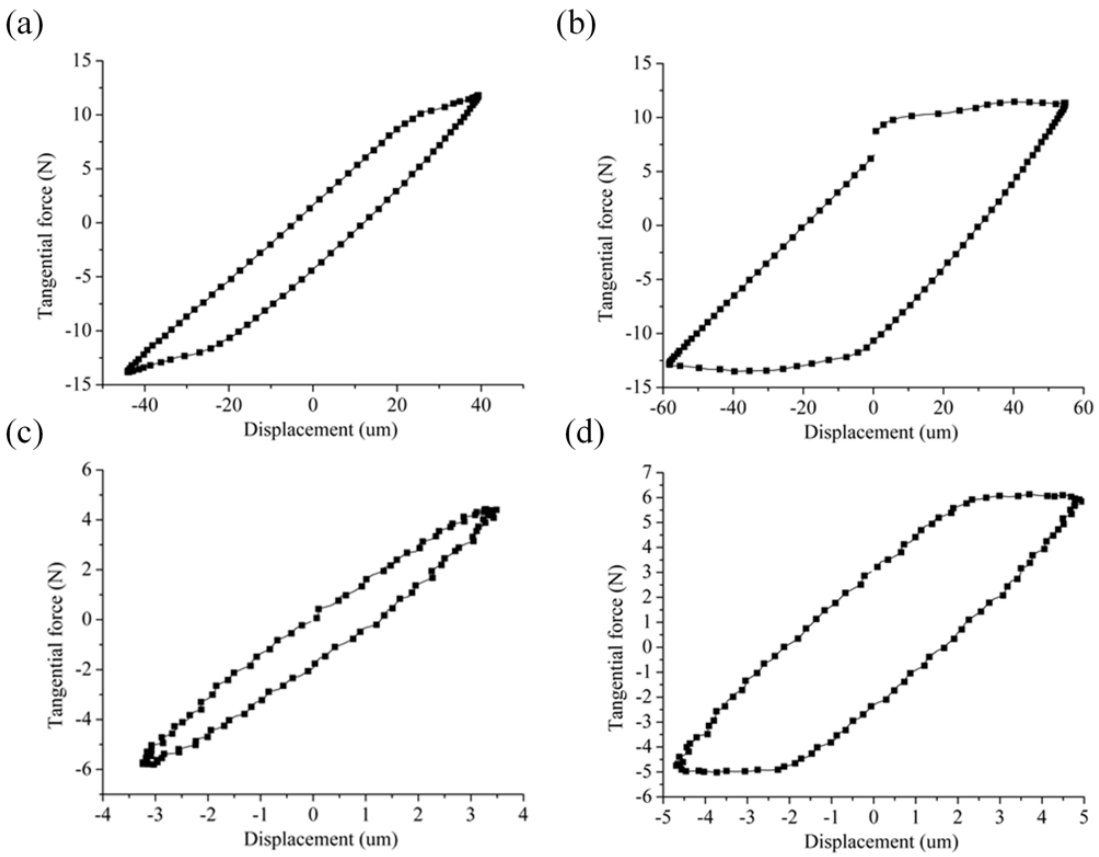

Figure 3

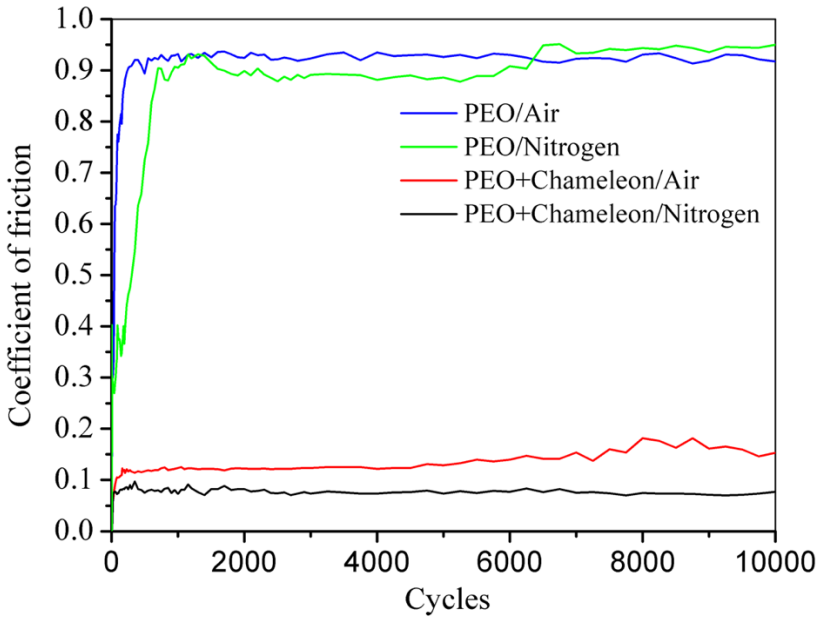

Figure 4

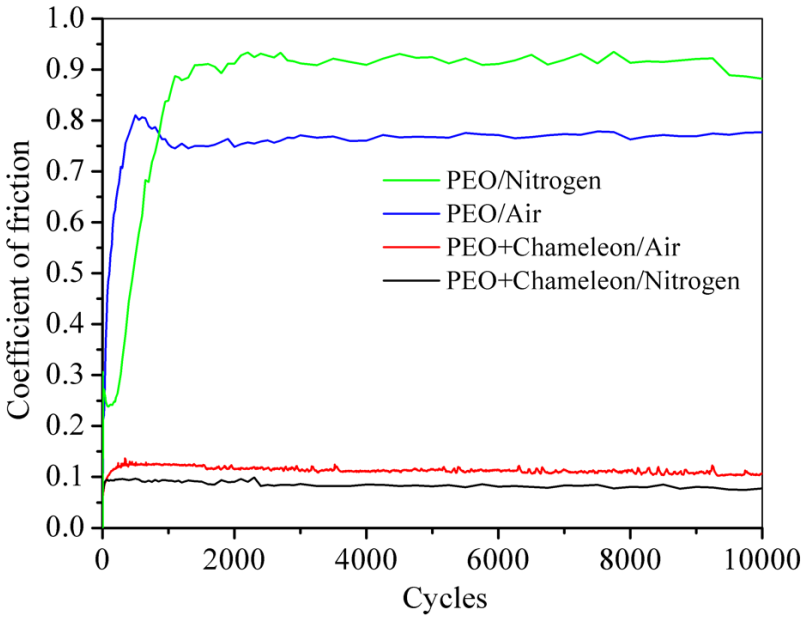

Figure 5

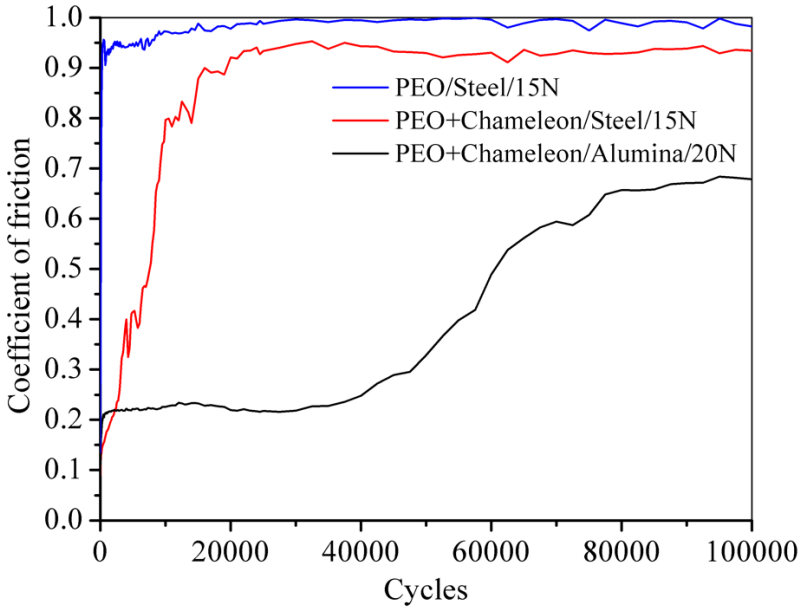

Figure 6

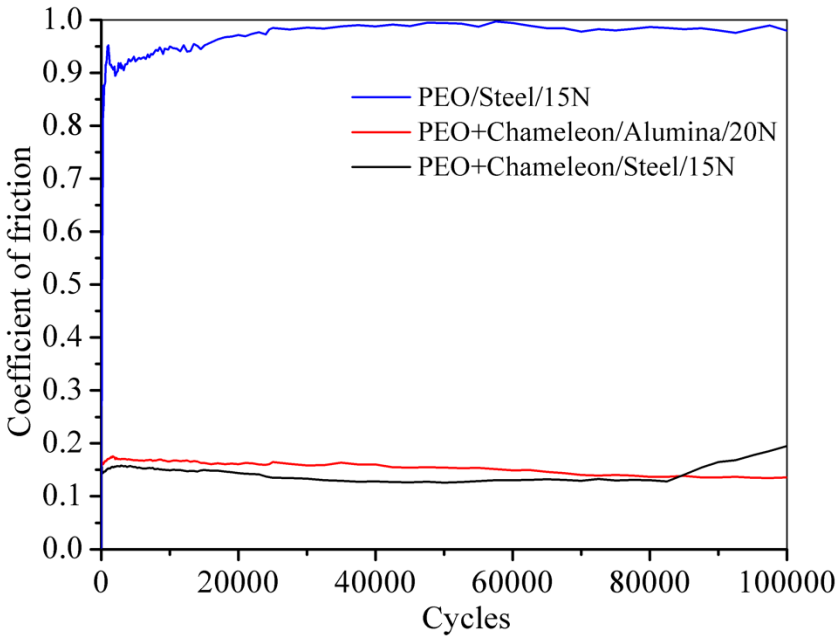

Figure 7

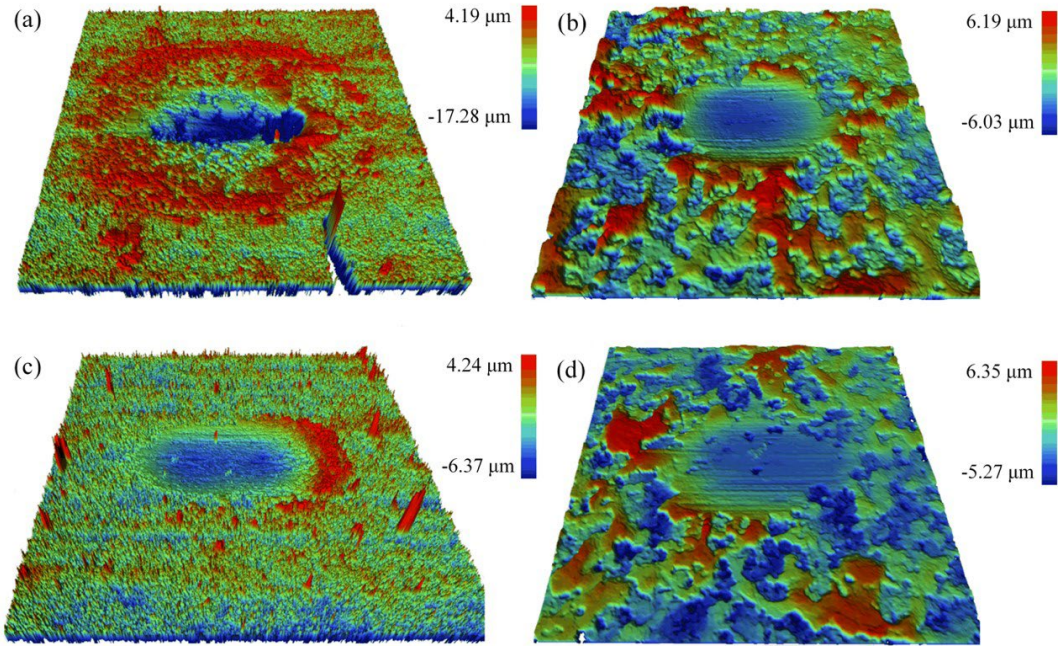

Figure 8

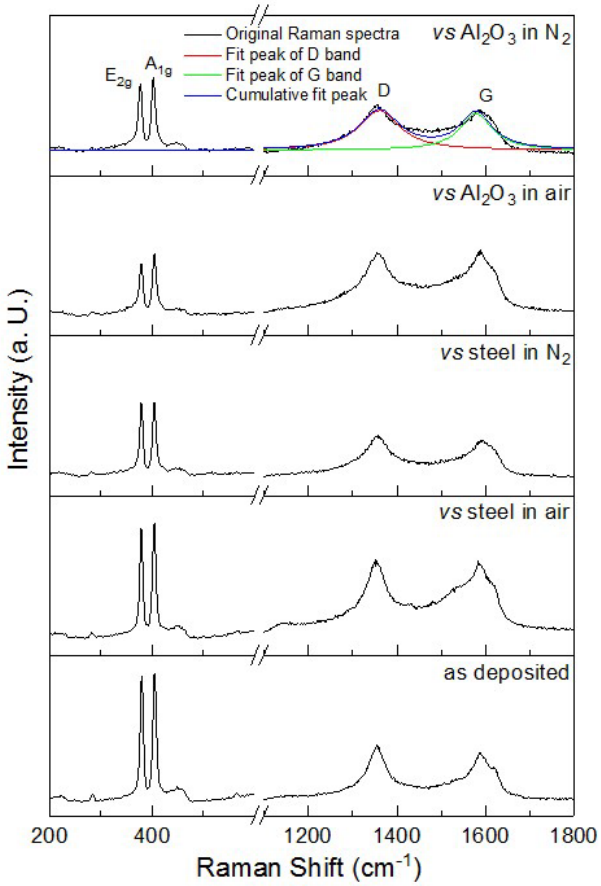
Original Raman spectra
Fit peak of D band
Fit peak of G band
Cumulative fit peak
E2g
A1g
D
G
vs Al2O3 in N2
vs Al2O3 in air
vs steel in N2
vs steel in air
as deposited
Intensity (a. U.)
200
400
1200
1400
1600
1800
Raman Shift (cm-1)

Figure 9